Electronic Supplementary Material (ESI) for New Journal of Chemistry.

Supplementary information

A simplified and cost-effective detection of cancer bio-marker using BODIPY and surfactant templated fluorogenic self-assembly

Soumyadeep Sarkar[a, b], Sudip Gorai[c,d], Akhilesh Potnis[e], Padma Nilaya Jonnalgadda[a,d], Soumyaditya Mula[c,d], Goutam Chakraborty[a]*

[a]Laser and Plasma Technology Division, Bhabha Atomic Research Centre, Mumbai-400085,

[b]On summer internship from IISER-K (Indian Institute of Science Education and Research, Kolkata), Campus Road, Mohanpur-741246, India.

[c]Bio-organic Division, Bhabha Atomic Research Centre, Mumbai-400085, India.

[d]Homi Bhabha National Institute, Anushaktinagar, Mumbai-400094, India.

[e]Molecular Biology Division, Bhabha Atomic Research Centre, Mumbai-400085, India.

Corresponding author: Goutam Chakraborty[a]*

[a]Laser and Plasma Technology Division, Bhabha Atomic Research Centre, Mumbai-400085, India.

E-mail: gchak@barc.gov.in (GC).

1. Experimental Section

A. Photophysical studies

All the UV-Vis and fluorescence spectroscopic studies were performed in UV-2700 spectrophotometer (Shimadzu, Japan) and Fluoromax-4 spectrofluorimeter (Horiba) respectively, taking the sample solutions in a quartz cuvette of 10 mm x 10 mm path length. Since, the change in absorbance for the dye at ~605 nm is significantly small during complexation process; in steady-state emission measurements all the sample solutions were excited at ~605 nm to mitigate any distortion in emission output. Temperature was kept constant (~25 ^{o}C) during all the spectroscopic investigations.

B. Dynamic light scattering (DLS)

Particle size analyzer (Model: SZ-100, Horiba, Japan) with a solid-state laser (532 nm wavelength and 10 mW power) pumped by diode, was utilized for the DLS measurements. The scattered light falling at an angle of 173^{o} on a photomultiplier provided the required signal. The measurements were carried out at least five successive times to have an average size of the aggregated particles. With the help of Stokes-Einstein's equation, hydrodynamic diameter (d_h) for the particles was evaluated, where, $D = k_B T/3\pi\eta d_h$ (where, k_B = Boltzman Constant, T= absolute temperature, D= diffusion coefficient, η = viscosity of solvent).

C. Atomic force microscopy (AFM)

Atomic Force Microscope (obtained from NTMDT Ntegra) was used to obtain AFM image of the BDP-Sty@SDS@Sp complex. The sample solution (10 μL) was spotted on a freshly cleaved mica plate of 1 cm x 1 cm dimension, attached to a sapphire substrate, and then gradually dried under an infrared lamp for ~30 minutes. The same was then placed on the sample holder of the AFM. Semi-contact mode was used to scan the mica surface with NSG11 golden silicon probe tip using a 100-micron scanner attached with a SMENA head. Measurements were done across X–Y–Z axis with the help of NTMDT NOVA 1.1.01780 software and which also measured the height of 50 randomly selected BDP-Sty@SDS@Sp particles using arbitrary height measurement tool.

D. Transmission electron microscopy (TEM)

For TEM, 10 μL of freshly prepared ternary complex, BDP-Sty@SDS@Sp was spotted on a carbon coated (Carbon Type-B, 200 mesh) Cu grid and then evaporated under infra-red lamp for about 45 minutes to make it completely dry. After that it was subjected to TEM study under transmission electron microscope (TEM) of Zeiss-Carl (Libra-120) at an accelerating voltage of 120 kV.

E. Calculation of limit of detection

Limit of detection (LOD) = $3\sigma/S$

where, σ = standard deviation, obtained from 10 successive fluorescence measurements of BDP-Sty@SDS binary complex (as blank) in buffer or in 20% urine or 0.5% human serum at λ_{ex} = 605 nm and S = slope of the calibration curve, obtained from the change in fluorescence intensity of the BDP-Sty@SDS binary complex as a function of spermine concentration.

F. Calculation of quantum yield (Φ)

Quantum yield of BDP-Sty in the form of free, binary (BDP-Sty@SDS) and ternary complex (BDP-Sty@SDS@Sp) were calculation using the following equation:

$$\frac{\boldsymbol{\Phi}_{Sam}}{\boldsymbol{\Phi}_{Std}} = \frac{FA_{Sam}}{FA_{std}} x \frac{OD_{Std}}{OD_{sam}} x \frac{\eta_{Sam}^2}{\eta_{Std}^2}$$

Where, Φ_{Sam} = Quantum yield of the species to be determined.

Φ_{Std} = Quantum yield of the standard = 0.04 for BDP-Sty in MeOH.[1]

FA_{sam} and OD_{sam} are the area under the fluorescence curve and optical density of the sample, respectively.

FA_{std} and OD_{std} are the area under the fluorescence curve and optical density of the standard, respectively.

η_{sam} = Refractive index of the medium of the sample = 1.333 (for aqueous medium)

η_{std} = Refractive index of the medium of the standard = 1.328 (for MeOH).

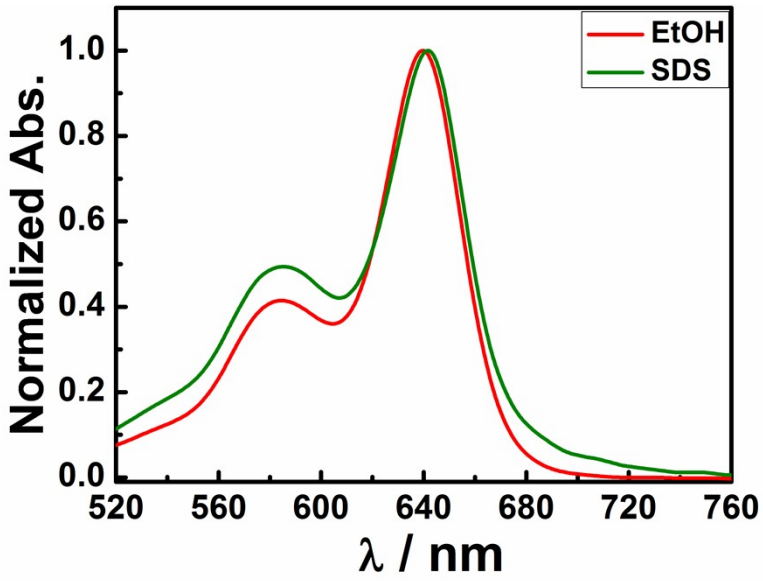

Figure S1. Normalized absorption spectra of BDP-Sty in EtOH (red) and in buffer solution containing 5 mM SDS (green).

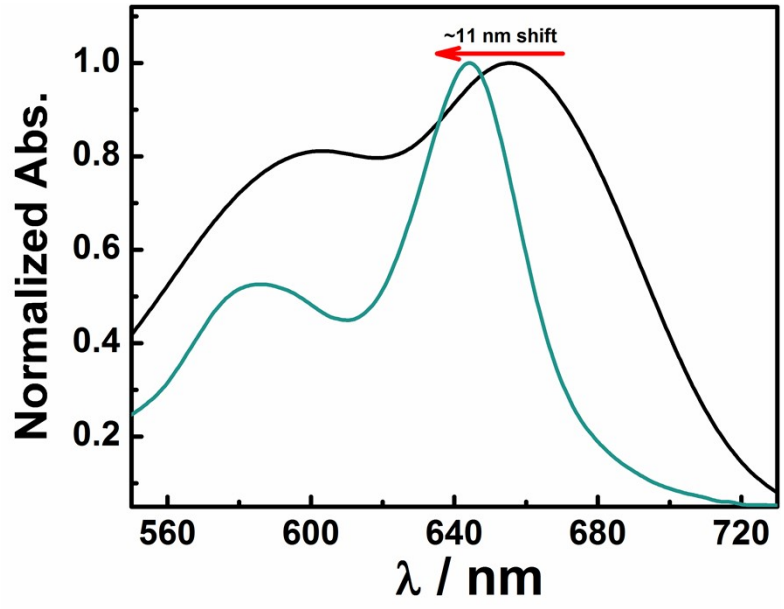

Figure S2. Normalized absorption spectra of BDP-Sty@SDS complex (3 μM BDP-Sty+0.6 mM SDS) at 0 (black) and 632.6 mM (green) of NaCl in 5 mM phosphate buffer at pH 7.

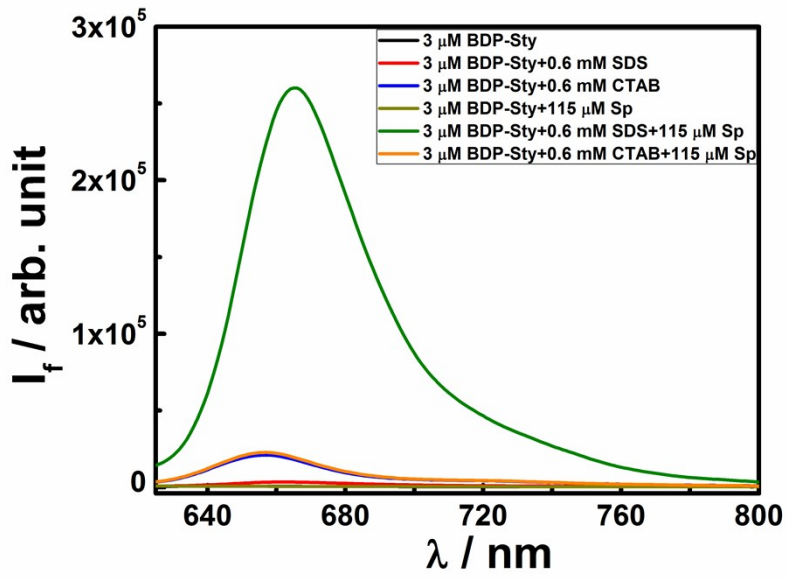

Figure S3. Emission spectra of 3 μM BDP-Sty at different combination in 5 mM phosphate buffer at pH 7. λ_{ex} = 605 nm.

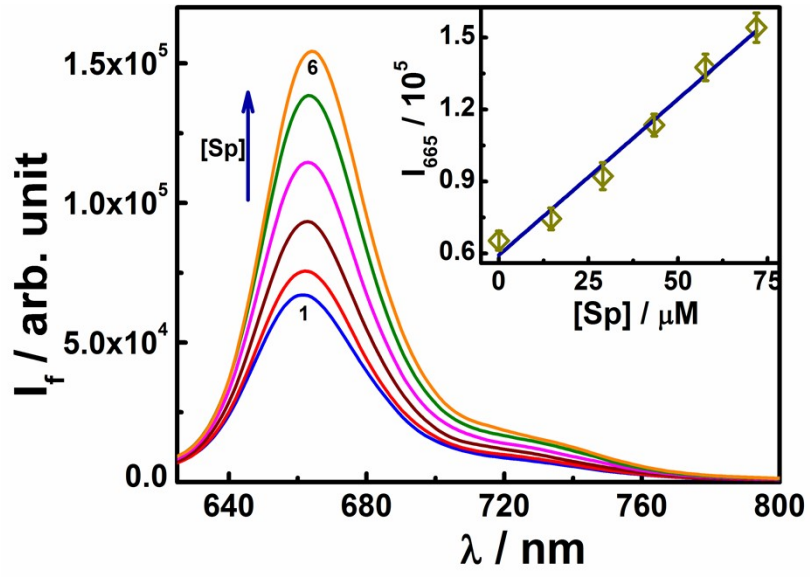

Figure S4. Emission spectra of BDP-Sty@PSS complex (3 μM BDP-Sty+2.5 μM PSS at (1) 0, (2) 14.5, (3) 29.0, (4) 43.4, (5) 57.7, and (6) 71.9 μM of Sp in 5 mM phosphate buffer at pH 7. **Inset:** Linear fit of intensity change of BDP-Sty@PSS complex with increasing spermine concentration. Linear regression is

I_{665} = 1.3 × 10^3 [Sp/μM] + 59365.2; R^2 = 0.982, LOD ~1.68 μM, standard deviation (σ) = 730.2. λ_{ex} = 605 nm.

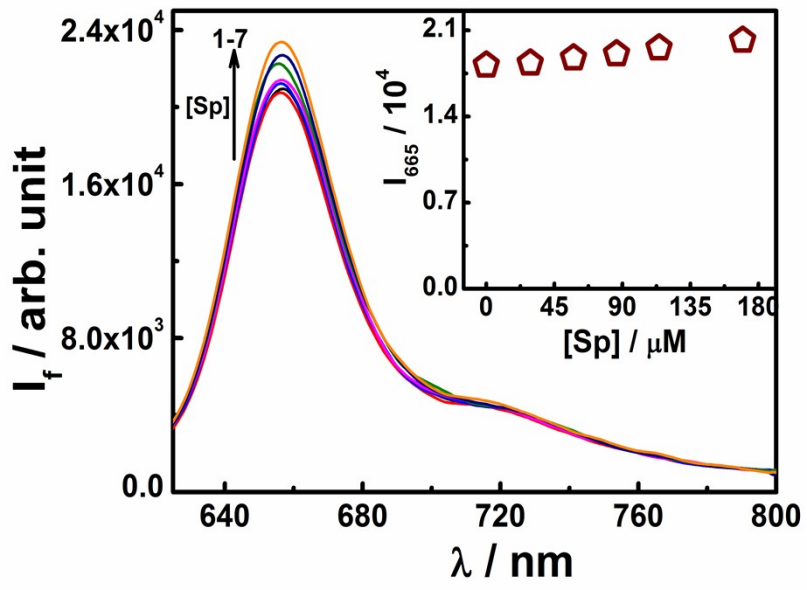

Figure S5. Emission spectra of BDP-Sty@CTAB complex (3 μM BDP-Sty+0.6 mM CTAB) at (1) 0, (2) 14.5, (3) 29.0, (4) 57.7, (5) 86.5, (6) 115.0 and (7) 169.6 μM of Sp in 5 mM phosphate buffer at pH 7. λ_{ex} = 605 nm.

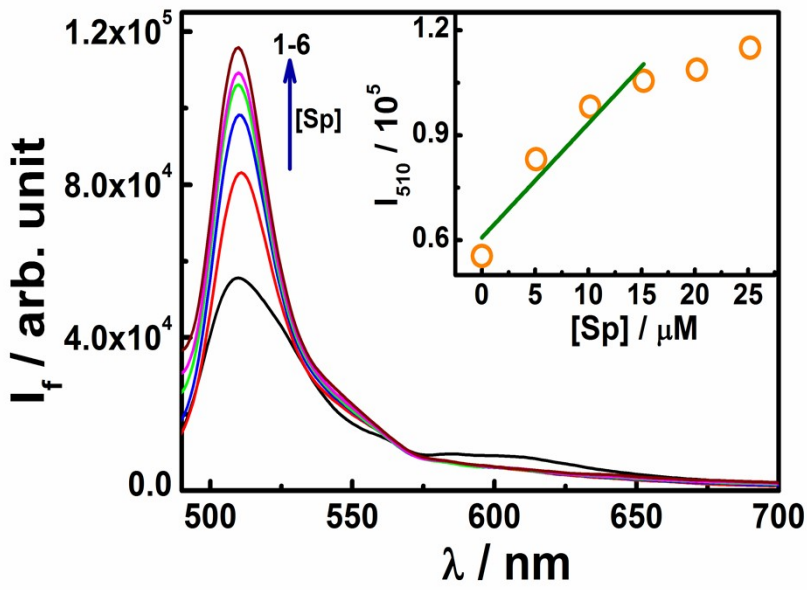

Figure S6. Emission spectra of BDP@SDS complex (3 μM BDP+0.6 mM SDS) at (1) 0, (2) 5.1, (3) 10.2, (4) 15.2, (5) 20.2 and (6) 25.2 μM spermine in 5 mM phosphate buffer at pH 7. λ_{ex} = 470 nm.

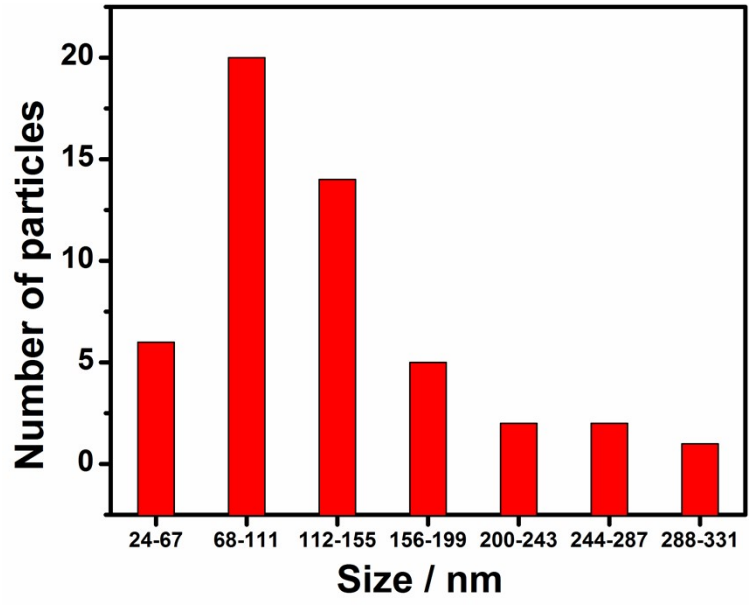

Figure S7. Size distribution of BDP-Sty@SDS@Sp ternary complex particles obtained from AFM study.

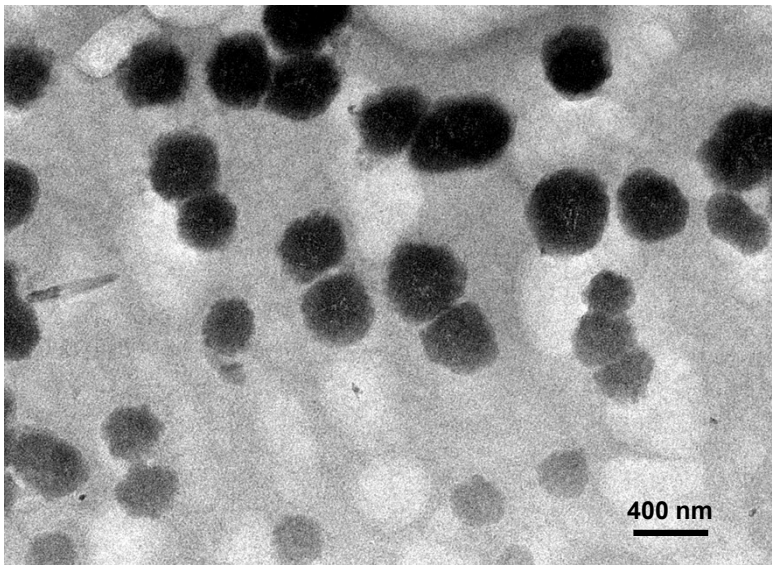

Figure S8. TEM image of BDP-Sty@SDS@Sp ternary complex particles obtained from AFM study.

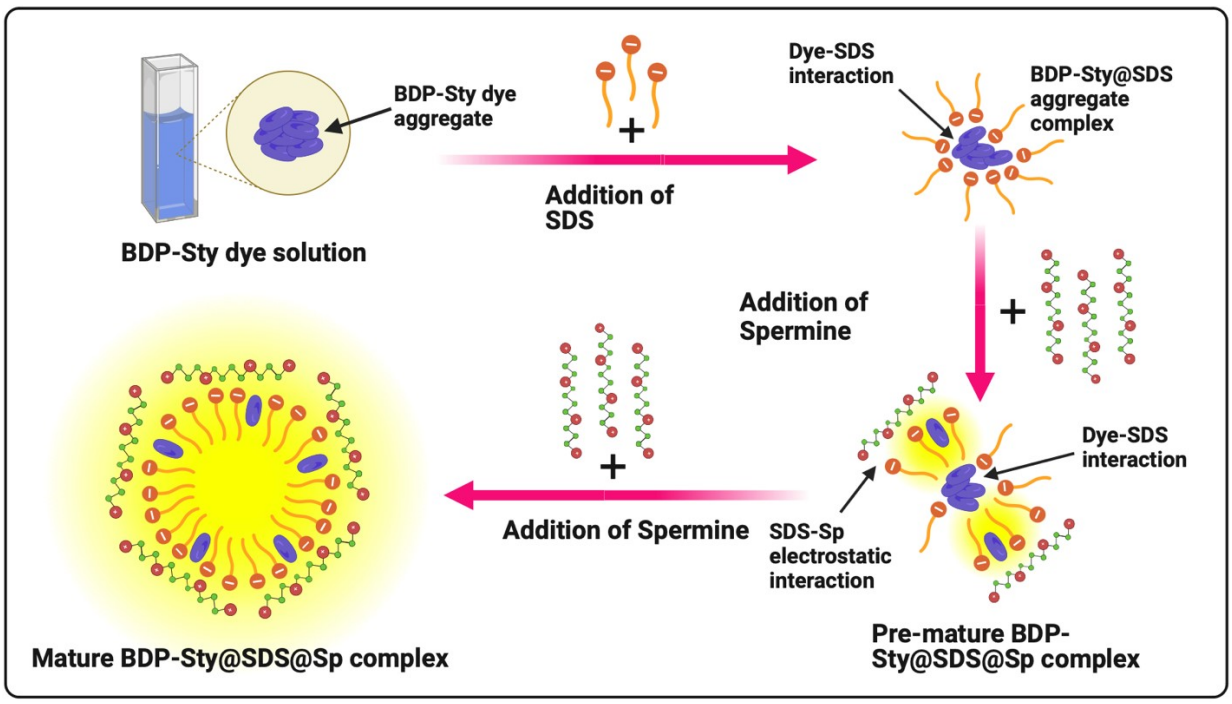

Figure S9. Schematic presentation of spermine detection by BDP-Sty@SDS binary complex.

Table S1. Quantum yield of BDP-Sty at different condition. Quantum yield (Φ) = 0.04 for BDP-Sty in MeOH has been taken as reference quantum yield for calculation.[1]

Species	Φ
BDP-Sty in MeOH	0.04
BDP-Sty in buffer	8.6×10^{-5}
BDP-Sty@SDS in buffer	1.2×10^{-4}
BDP-Sty@SDS@Sp in buffer	0.004

Table S2. Different optical probes used for spermine detection.

S.N.	Probes	Dynamic Range	Limit of detection (LOD)	Reference
1.	Metal-mediated ethynylarene	25 μM – 2.5 mM	25 μM	2
2.	Mixture of anionic pyrocatechol violet (PV) and 3-carboxyphenylboronic acid (CPB)	1–10 μM	6.24 μM	3
3.	Hydrogel CB@AG	6 μM–2.5 mM	6 μM	4
4.	POC12-SQ Complex	20–100 μM	4.73 μM	5
5.	Carboxylic acid-functionalized polyfluorene (PFCOOH-BT5)	0–20 μM	2 μM	6
6.	Supramolecular Hydrogel Hybrid of G-coum⊂MMT	20–100 μM	1.4 μM	7
7.	Selective AIE-CB7 based fluorescent probes	0–12 μM	1.0 μM	8
8.	Tetraphenylethylene derivative based probe	1–31 μM	0.7 μM	9
9.	Self-assemblies ENS-1 and ENS- 2	0–2.5 μM and 0–20 μM	6 nM and 0.5 μM	10
10.	Ciprofloxacin-Tb^{3+} complex	2–180 μM	0.17 μM	11
11.	BDP-Sty@SDS assembly	0–75 μM in buffer, 0–96 μM in 50% urine and 0–66 μM in 0.5% serum	65.6 nM in buffer, 1.79 μM in 50% urine and 2.38 μM in 0.5% human serum	**This work**

References:

1. S. Gorai, S. Mula, P. N. Jonnalgadda, B. S. Patro and G. Chakraborty, *Talanta*, 2023, **265**, 124915.

2. J. T. Fletcher and B. S. Bruck, *Sens. Actuators, B*, 2015, **207**, 843-848.

3. Y. Fukushima and S. Aikawa, *Microchem. J.*, 2021, **162**, 105867.

4. R. R. Nair, S. Debnath, S. Das, P. Wakchaure, B. Ganguly and P. B. Chatterjee, *ACS Appl. Bio Mater.*, 2019, **2**, 2374-2387.

5. J. Tu, S. Sun and Y. Xu, *Chem. Commun.*, 2016, **52**, 1040–1043.

6. B. Bao, L. Yuwen, X. Zheng, L. Weng, X. Zhu, X. Zhan and L. Wang, *J. Mater. Chem.*, 2010, **20**, 9628-9634.

7. M. Ikeda, T. Yoshii, T. Matsui, T. Tanida, H. Komatsu and I. Hamachi, *J. Am. Chem. Soc.*, 2011, **133**, 1670-1673.

8. G. Jiang, W. Zhu, Q. Chen, X. Li, G. Zhang, Y. Li, X. Fan and J. Wang, *Sens. Actuators, B*, 2018, **261**, 602-607.

9. M. Barros, S. Ceballos, P. Arroyo, J. A. Sáez, M. Parra, S. Gil, A. M. Costero and P. Gaviña, *Chemosensors*, 2022, **10**, 8.

10. N. Tripathi, P. Singh, V. Luxami, D. Mahajan and S. Kumar, *Sens. Actuators, B*, 2018, **270**, 552-561.

11. N. Ngoc Nghia, B. The Huy, P. Thanh Phong, J. S. Han, D. H. Kwon and Y.-I. Lee, *PLoS ONE*, 2021, **16**, e0251306.